J. Plasma Physics (1999), *vol.* 61, *part* 3, *pp.* 415–423. Printed in the United Kingdom
© 1999 Cambridge University Press

Collisionless magnetic reconnection in the presence of an external driving flow

RITOKU HORIUCHI and TETSUYA SATO

Theory and Computer Simulation Center, National Institute for Fusion Science, 322-6 Oroshi-cho, Toki, Gifu 509-5292, Japan

(Received 1 June 1998 and in revised form 10 November 1998)

The dynamical development of collisionless reconnection and the consequent energy-conversion process in the presence of an external driving flow are investigated by means of a full particle simulation. Magnetic reconnection develops in two steps in accordance with the formation of ion and electron current layers. In the early phase magnetic reconnection is controlled by an ion kinetic effect, while an electron kinetic effect becomes dominant in the late phase. There exist two mechanisms associated with the particle kinetic effects, that break the frozen-in condition of magnetic field and lead to magnetic reconnection in a collisionless plasma, namely a particle inertia effect and a particle thermal orbit effect. It is found that the dominant triggering mechanism in the late phase changes from an electron thermal orbit effect to an electron inertia effect as the longitudinal magnetic field increases. Electron acceleration and heating take place in the reconnection area under the influence of the reconnection electric field, while the energy conversion takes place from electrons to ions through the action of an electrostatic field excited downstream. As a result, the average ion temperature becomes about 1.5 times the average electron temperature.

1. Introduction

Driven magnetic reconnection (Sato and Hayashi 1979; Sato et al. 1992) is an interesting and important process, because it can lead to fast energy conversion from an electromagnetic field to particles, as well as a change in the topology of the magnetic field. Magnetic reconnection, however, cannot take place in an ideal magnetohydrodynamic plasma, because the magnetic field is frozen in the plasma. This means that a non-ideal effect, that breaks the frozen-in condition and leads to the generation of an electric field along an equilibrium current is needed for the excitation of magnetic reconnection.

In two-dimensional systems there exist two types of microscale particle kinetic effects responsible for the decoupling of the magnetic field from particle motion in a collisionless plasma (Horiuchi and Sato 1994, 1997). One is the particle inertia effect, which becomes significant on a spatial scale comparable to the collisionless skin depth. The other is the particle orbit effect, which becomes effective on an excursion scale of particle thermal motion, which is called meandering motion. In principle the particle thermal orbit effect is equivalent to the finite-Larmor-radius (FLR) effect. On the other hand, because there are two species of charged particles in a plasma, namely ions and electrons, particle kinetic effects can be classified into

ion effects and electron effects. In other words, there are two classes of particle kinetic effects. For example, the particle thermal orbit effect consists of an ion FLR effect and an electron FLR effect. In this paper we shall clarify which of these effects can play a leading role in collisionless reconnection by examining the dynamical process of collisionless reconnection for the case where the system is subjected to an external driving flow, i.e. 'collisionless driven reconnection'.

2. Simulation model

Let us consider a two-dimensional open system where physical quantities are translationally symmetric in the z-direction ($\partial/\partial z = 0$). The simulation is carried out using a $2\frac{1}{2}$-dimensional electromagnetic, full particle code (Birdsall and Langdon 1985; Horiuchi and Sato 1994, 1997). Because both ions and electrons are treated as particles, not only the ion FLR effect but also the electron FLR effect can be described in this simulation code. As an initial condition we adopt a one-dimensional equilibrium with a sheared magnetic field as

$$\mathbf{B}(y) = \left(B_0 \tanh\frac{y}{L}, 0, B_{z0} \right), \tag{2.1}$$

$$P(y) = \frac{B_0^2}{8\pi} \operatorname{sech}^2 \frac{y}{L}, \tag{2.2}$$

where B_0 and B_{z0} are constants and L is the scale height along the y axis. The initial particle distribution is given by a shifted Maxwellian with a spatially constant temperature ($T_i = T_e$) and the average particle velocity is equal to the diamagnetic drift velocity.

It is assumed here that physical quantities are periodic at the boundary of the x axis ($x = \pm x_b$) and that there is a driving electric field at the boundary of the y axis ($y = \pm y_b$) in order to supply the plasma with the $\mathbf{E} \times \mathbf{B}$ drift velocity into the simulation domain. The electrostatic field is assumed to be zero at the input boundary, because both an ion and an electron are loaded to the same spatial position near the input boundary with the same rate determined by the $\mathbf{E} \times \mathbf{B}$ drift velocity. The driving electric field is determined so as to be always normal to both the magnetic field and the input flow velocity. The amplitude of driving electric field $E_{d0}(x, t)$ is taken to be zero at $t = 0$ and gradually increases for some initial period. After this period, $E_{d0}(x, t)$ is described by a symmetric constant profile with a maximum input rate of magnetic flux E_0 at the centre of the input boundary. We discuss the simulation results for the case of $E_0 = -0.04B_0$ in this paper.

3. Two-step evolution of collisionless driven reconnection

Charged particles execute a complex thermal motion, which is called meandering motion, in the vicinity of a magnetically neutral sheet (Horiuchi and Sato 1990). The average orbit amplitude of meandering motion is given by $l_{m\alpha} = (\rho_\alpha L)^{1/2}$ for $B_{z0} = 0$, where ρ_α is the Larmor radius of a charged particle of species α (Horiuchi and Sato 1994). In this section we discuss the relationship between the ion thermal effect and the electron thermal effect for the case of $B_{z0} = 0$, where both the ion and electron meandering (thermal) scales are much longer than the collisionless skin depth (an electron inertia scale). Four snapshots of magnetic flux contours in the (x, y) plane are shown in Fig. 1. The plasmas are supplied to the system through the top

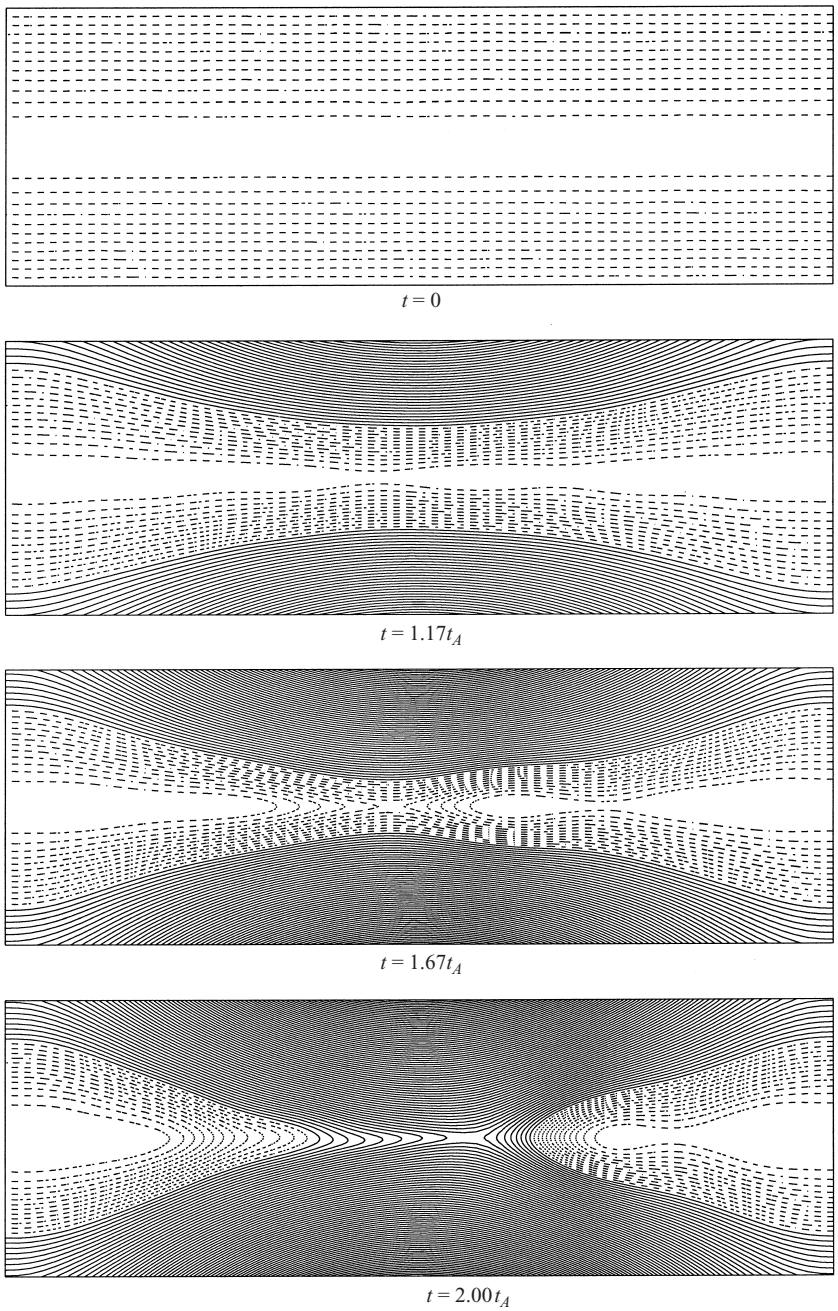

Figure 1. Temporal evolutions of magnetic flux contours in the (x, y) plane for the case $B_{z0} = 0$. Solid lines indicate the magnetic flux supplied into the system through the top and bottom boundaries.

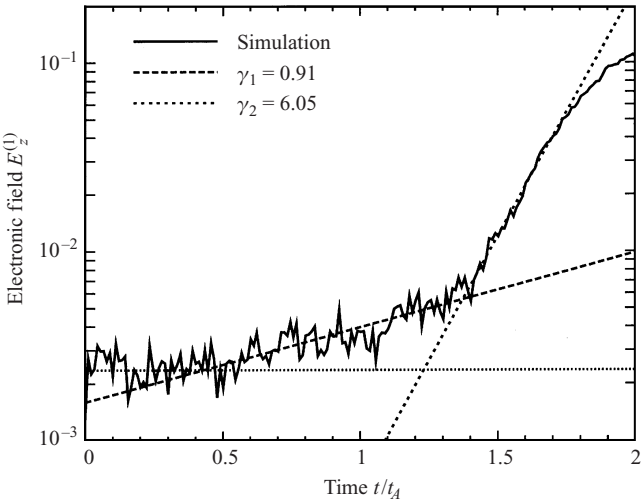

Figure 2. Temporal evolution of reconnection electric field for the case $B_{z0} = 0$.

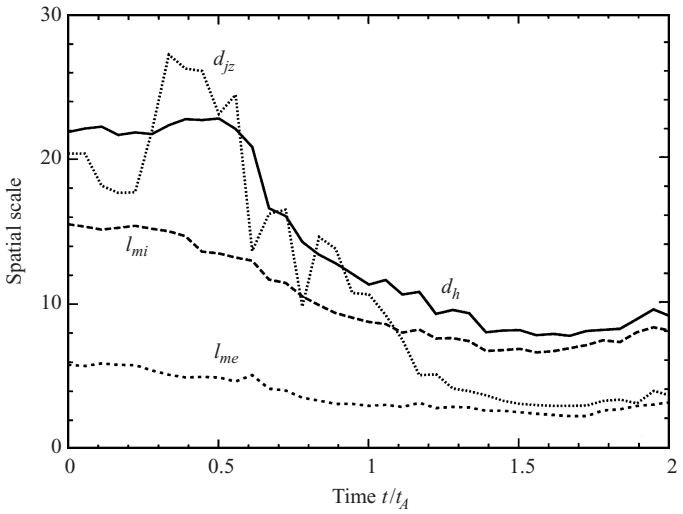

Figure 3. Temporal evolutions of four spatial scales for the case $B_{z0} = 0$.

and bottom boundaries. The current layer is compressed by the convergent plasma flow, and thus its width decreases with time. Magnetic reconnection takes place at the centre of the current layer, and the reconnected flux is carried away towards the downstream (the left and right boundaries) by the fast divergent plasma flow.

Let us examine the behaviours of two meandering scales and an electric field along the equilibrium current at the reconnection point, i.e. the 'reconnection electric field'. Figures 2 and 3 show the temporal evolution of the reconnection electric field $E_z^{(1)}$, and those of four spatial scales, where d_h, d_{jz}, l_{mi} and l_{me} are the half-width of the mass density profile, the half-width of the current density profile, the average orbital amplitude of ion meandering motion and the average orbital amplitude of electron meandering motion respectively. The electric field begins to grow slowly

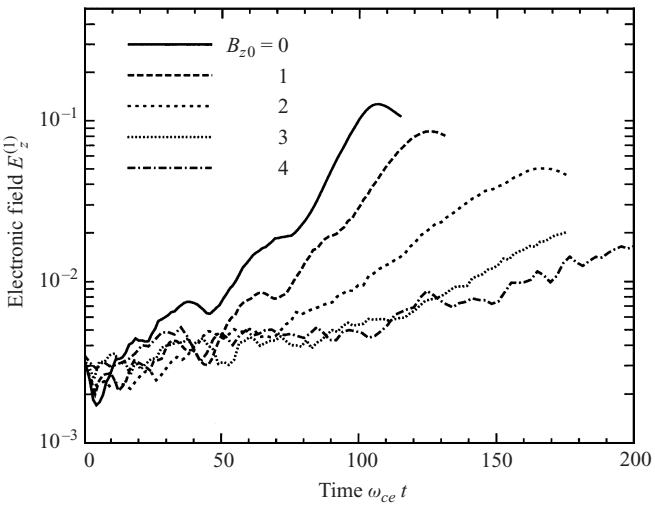

Figure 4. Temporal evolution of the reconnection electric field for five different values of B_{z0}, where the longitudinal field B_{z0} is normalized by the asymptotic value of the reconnection field B_0.

as soon as both d_h and d_{jz} start to decrease as a result of the compression by the convergent plasma flow in the slow-reconnection phase ($0.6t_A < t < 1.3t_A$). The width of the current layer is almost the same as or a little larger than the ion thermal scale l_{mi} in this phase. Because most of the ions are unmagnetized in the current layer (the 'ion current layer'), while the electrons are magnetized, the input flow (Poynting flux) no longer acts to thin the ion current layer, but it continues to compress the electron profile. Thus an electron current layer is created inside the ion current layer owing to the finite-ion-Larmor radius effect. When the fast-reconnection phase ($1.3t_A < t < 1.8t_A$) sets in, the inclination of the growth curve steepens suddenly and the half-width of the electron current layer approaches the electron thermal scale l_{me}. These results lead us to the conclusion that the slow reconnection is triggered by the ion thermal orbit effect while the fast reconnection is triggered by the electron thermal orbit effect.

4. Reconnection mechanism

There exist two mechanisms, associated with particle kinetic effects, that lead to magnetic reconnection in a collisionless plasma, namely the particle inertia effect and the particle thermal effect. The thermal motion of charged particles becomes magnetized and its spatial scale decreases as the longitudinal magnetic field increases (Horiuchi and Sato 1997). This means that the relationship between the particle thermal (meandering) scale and the particle inertia scale changes with the magnetic field. In this section we clarify the role of the two mechanisms in collisionless reconnection by examining the simulation results for different values of B_{z0}. The influence of the longitudinal magnetic field B_{z0} on the behaviour of the reconnection electric field is shown in Fig. 4. One can see that both the growth rate and the saturation value of the reconnection electric field decrease as the longitudinal field becomes stronger. This result can be explained as follows. When the current layer is compressed as thin as the ion kinetic scale, the coupling between the

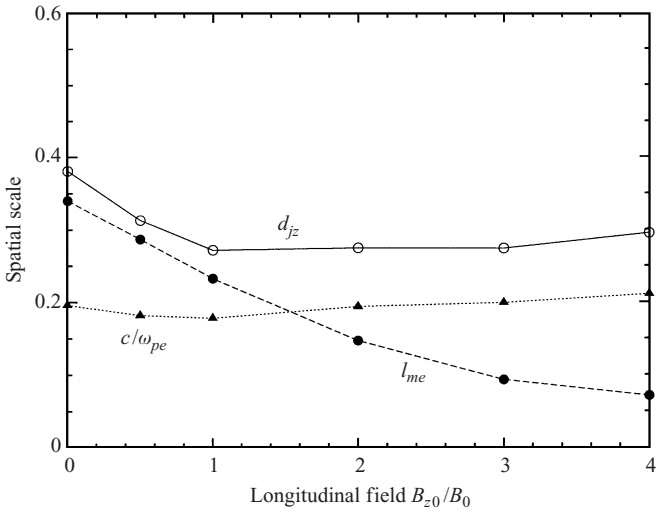

Figure 5. Dependence of three spatial scales on a longitudinal field for the electron phase.

ions and the magnetic field is broken and the magnetic flux can penetrate into the current layer with the $\mathbf{E} \times \mathbf{B}$ velocity (Fruchtman and Gomberoff 1993). Magnetic reconnection is triggered when this convective electric field carried by the $\mathbf{E} \times \mathbf{B}$ drift motion reaches the centre of the current layer. The reconnection electric field grows while satisfying the balance condition between the flux input rate and the reconnection rate. Because the flux input rate is proportional to $[1+(B_{z0}/B_0)^2]^{-1/2}$, the reconnection electric field grows more slowly as B_{z0} increases.

Figure 5 illustrates the dependence of three spatial scales on the field ratio B_{z0}/B_0 when the current layer becomes thinnest in the fast-reconnection phase (the electron phase). The width is nearly equal to l_{me} and two times as large as c/ω_{pe} for $B_{z0} = 0$. The electron thermal motion becomes strongly magnetized and its spatial scale l_{me} decreases as B_{z0} increases. On the other hand, the skin depth (the electron inertia scale) is almost independent of B_{z0}/B_0. Thus the relation $l_{me} < c/\omega_{pe}$ holds for $B_{z0} > 1.5B_0$. In other words, the electron inertia scale is longer than the electron thermal scale for a strong field $B_{z0} > 1.5B_0$. It can be clearly seen from Fig. 5 that the width d_{jz} decreases with l_{me} until l_{me} reaches c/ω_{pe}. For $l_{me} < c/\omega_{pe}$, the width ceases to decease, and exhibits the same behaviour as c/ω_{pe}. This means that collisionless driven reconnection in the fast reconnection phase proceeds while keeping the width of current layer nearly equal to the electron skin depth for a strong longitudinal field $B_{z0} > 1.5B_0$. Thus the triggering mechanism for collisionless driven reconnection in the fast-reconnection phase changes from the electron thermal effect to the electron inertia effect in accordance with increasing B_{z0}.

5. Energy conversion by the electric field

Energy conversion between an electromagnetic field and particles takes place through the work done by the electric field in the plasma, i.e. $\mathbf{E} \cdot \mathbf{j}$. Let us decompose the electric field into the electromagnetic component $\mathbf{E}_{mg}$ and the electrostatic component $\mathbf{E}_{st}$, and the electric current $\mathbf{j}$ into the ion current $\mathbf{j}_i$ and the electron current $\mathbf{j}_e$, in order to obtain detailed information about the energy-conversion

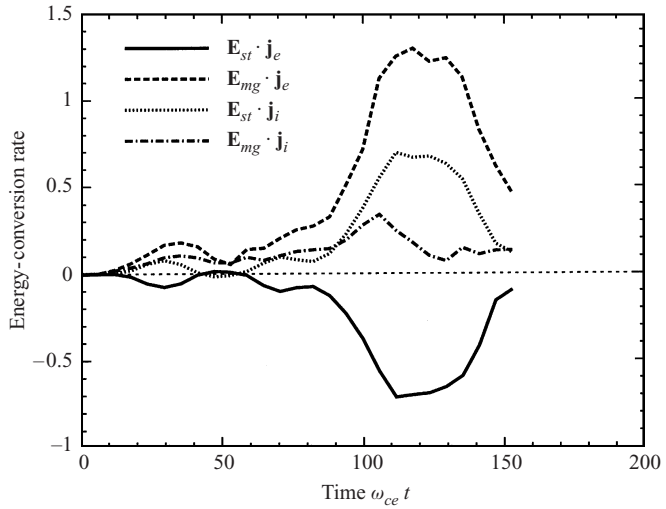

Figure 6. Temporal evolutions of four components of the energy-conversion rate for the case $B_{z0} = 0$.

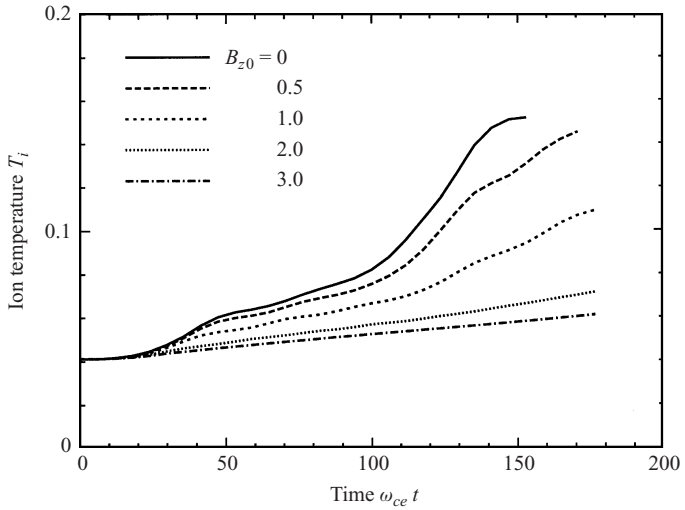

Figure 7. Temporal evolutions of the average ion temperature for the same cases as in Fig. 4.

process. Figure 6 shows the temporal evolutions of four components of the energy-conversion rate for the case $B_{z0} = 0$. One can see an interesting feature in Fig. 6, namely that two conversion rates by the electrostatic field, $\mathbf{E}_{st} \cdot \mathbf{j}_i$ (dotted curve) and $\mathbf{E}_{st} \cdot \mathbf{j}_e$ (solid curve), exhibit very similar behaviour except that the ion rate is always positive and the electron rate is always negative. Detailed examination reveals that the electromagnetic component acts on the particles in the vicinity of the reconnection point and leads mainly to an increase in the electron energy ($\mathbf{j}_e \cdot \mathbf{E}_{mg}$), while the electrostatic field becomes significant at the shock-like region downstream, and leads to fast energy conversion from electrons to ions through ambipolar interaction ($\mathbf{j}_e \cdot \mathbf{E}_{st} < 0$, $\mathbf{j}_i \cdot \mathbf{E}_{st} > 0$). Consequently, the average ion tem-

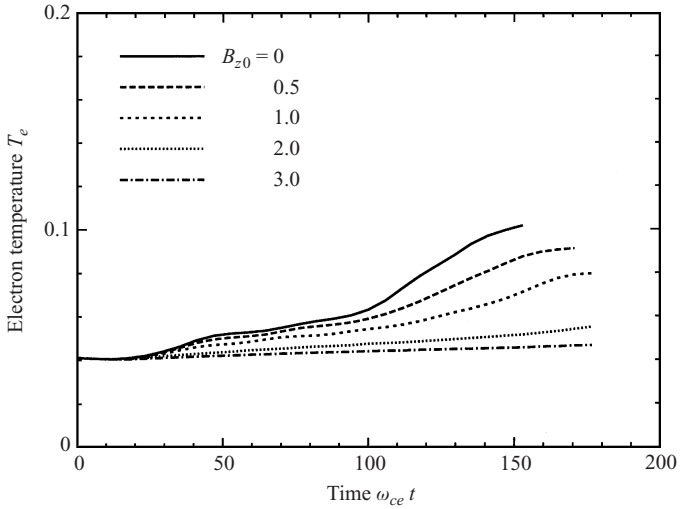

Figure 8. Temporal evolutions of the average electron temperature for the same cases as in Fig. 4.

perature increases to about 1.5 times the average electron temperature through collisionless driven reconnection, as shown in Figs 7 and 8. Here the average is taken over the whole simulation domain. We can also see in Figs 7 and 8 that the energy conversion occurs more actively in a plasma without any longitudinal magnetic field, and its rate decreases with B_{z0}.

6. Summary

The dynamical development of collisionless driven reconnection and the consequent energy-conversion process in sheared magnetic fields have been investigated by means of a $2\frac{1}{2}$-dimensional particle simulation. Magnetic reconnection develops in two steps in accordance with the formation of ion and electron current layers. The dominant triggering mechanism for electron phase changes from the electron thermal effect to the electron inertia effect as the longitudinal magnetic field increases. It is also found that energy conversion from electrons to ions takes place through the action of an electrostatic field excited downstream, and thus the average ion temperature becomes about 1.5 times the average electron temperature for no longitudinal magnetic field.

References

Birdsall, C. K. and Langdon, A. B. 1985 *Plasma Physics via Computer Simulation*. McGraw-Hill, New York.

Fruchtman, A. and Gomberoff, K. 1993 Magnetic field penetration due to the Hall field in (almost) collisionless plasmas. *Phys. Fluids* **B5**, 2371–2377.

Horiuchi, R. and Sato, T. 1990 The meandering orbit effect on stabilization of the tilting instability in a field-reversed configuration. *Phys. Fluids* **B2**, 2652–2660.

Horiuchi, R. and Sato, T. 1994 Particle simulation study of driven magnetic reconnection in a collisionless plasma. *Phys. Plasmas* **1**, 3587–3597.

Horiuchi, R. and Sato, T. 1997 Particle simulation study of collisionless driven reconnection in a sheared magnetic field. *Phys. Plasmas* **4**, 277–289.

Sato, T. and Hayashi, T. 1979 Externally driven magnetic reconnection and powerful magnetic energy converter. *Phys. Fluids* **22**, 1189–1202.

Sato, T., Hayashi, T., Watanabe K., Horiuchi, R., Tanaka M., Sawairi N. and Kusano, K. 1979 Role of compressibility on driven magnetic reconnection. *Phys. Fluids* **B4**, 450–457.